Residual Austenite and its Effect on Fracture Toughness of Coarse-Grained Heat-Affected Zone of H.S.L.A. Steels.

R. Taillard, J. Poct, Métallurgie Physique, Université de Lille I, Villeneuve d'Ascq, France.
P. Verrier, T. Maurickx, Centre de Recherches et de Développements Métallurgiques, Sollac, Dunkerque, France.

Introduction

Structural steels are used in ever more severe environment. In order to overcome this difficulty, the steels must satisfy requirements in the base metal and in the weldments. One of the most critical properties is a high toughness, at low temperatures, in the coarse-grained heat-affected zone (H.A.Z.). The aim of the present paper is to investigate the effect of the microstructure, and more particularly of the residual austenite content, on the H.A.Z. resilience in low carbon microalloyed steels. By the way, the volume fraction and composition of the austenite are determined by X-ray diffractometry and Mössbauer spectrometry.

Materials and experimental procedures

The base composition of the seven microalloyed steel specimens is 0.1 wt % C, 1.5 wt % Mn, 0.4 wt % Ni and 0.050 wt % Al. Table I exhibits the composition variations between the alloys. The only Ti-microalloyed steels VI and VII were produced using a controlled rolling and accelerated cooling process. The steels I to V arise from controlled rolling and normalisation treatments. It is worth noting that they differ by their level in microalloying additions. Steel I contains V, Nb and Ti whereas steel II displays Nb and Ti and steel III only Nb. Alloys IV and V are only Ti-microalloyed.

Steel	C	Si	V	Nb	Ti	N
I	100 / 110	450 / 500	32	28	15	4
II			-	26	13	3
III			3	34	-	4
IV			-	-	20	3
V			-	-	10	4
VI	89		-	-	11	2
VII	90	275	-	-	8	3

Tab. 1: Chemical analysis (10^{-3} wt %) of the steels plates.

The steels were investigated after simulated H.A.Z. thermal cycles. These heat treatments were applied using a Gleeble

1500 thermomechanical simulator. The cycles were defined by a 400K.s^{-1} heating rate up to 1623 K (1350°C) and by a cooling time (Δt) between 973 K (700°C) and 573 K (300°C). The cooling rate depends on welding energy. For the steels II, IV and V the Δt is equal to 300 s (10 kJ.mm^{-1}) whereas it is ranging from 10 to 300 s (0.3 kJ.mm^{-1} to 10 kJ.mm^{-1}) for the other alloys. The width of the simulated H.A.Z. is close to 5 mm.
The microstructural analyses were performed by X-ray diffractometry, thin foil (45 µm) transmission Mössbauer spectrometry, light, scanning and thin foil transmission electron microscopy.
The mechanical properties were characterized by instrumented Charpy V toughness and C.T.O.D. tests. These experiments were carried out with specimens which were taken in transverse direction and close to the plate surfaces. Dimensions of the C.T.O.D. samples were 20x10x100 mm with total notch and crack length of 10 mm including 2 mm fatigue crack.

Results and discussion

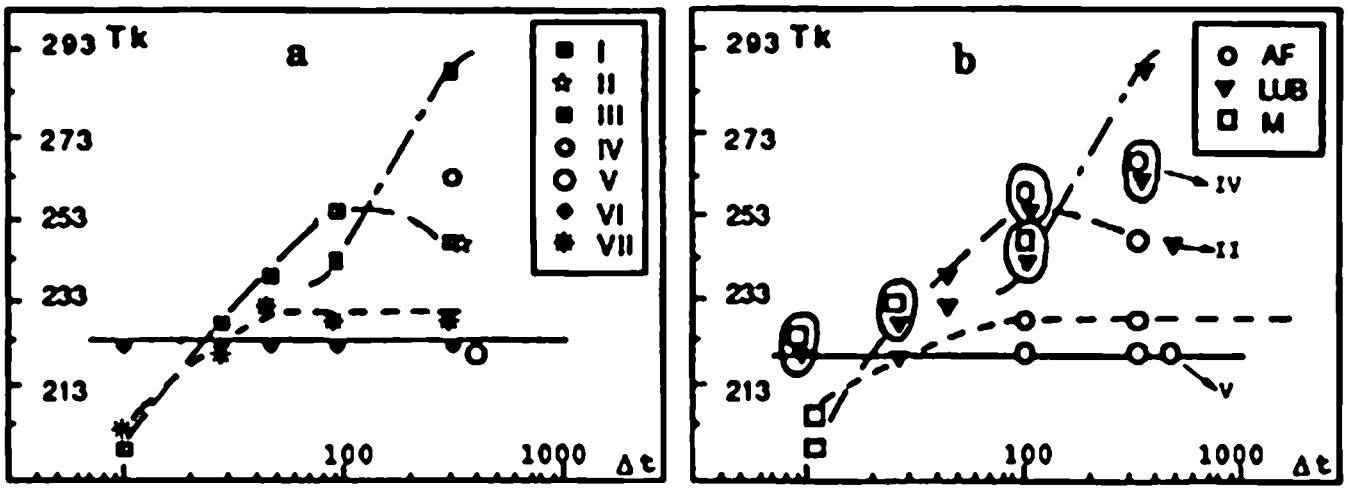

Fig. 1: Evolution of T_K with Δt : a) Experimental data, b) correlation with microstructure (M : martensite, L.U.B. : lath upper bainite, A.F. : acicular ferrite)

Fig. 1 exhibits the relationship between the 28 J Charpy V transition temperatures (T_K) of the materials and their heat treatment. It is worth noting that, except for steel VI for which T_K remains constant, T_K increases in general way with the welding energy. Furthermore, the chemical composition dependence of T_K is noticeable at all Δt. These features are explained by the H.A.Z. microstructure differences.

1. H.A.Z. microstructure

The percentages of H.A.Z. phases contents are collected in Tab. 2. Representative micrographs of the various phases have already been published (1-4). With the increment of Δt, the microstructure changes from martensite, to lower bainite, lath upper bainite and finally to a mixture of acicular and proeutec-

toïd ferrite. The differences in proeutectoïd ferrite, lath upper bainite and acicular ferrite volume fractions among the various alloys pertain to their levels of nitrogen and of micro-alloying additions (V,Ti,Nb) (2-3). Moreover, and as illustrated by Fig. 2, transmission electron microscopy shows the presence of "Martensite-Austenite-Carbide" (M.A.C.) second phases in upper bainite.

	I				II	III				IV	V	VI				VII			
Δt	10	30	100	300	300	10	30	100	300	300	300	10	30	100	300	10	30	100	300
M	70	50	-	-	-	100	95	50	-	-	-	55	35	-	-	80	55	-	-
LUB	30	50	50	5	85	-	5	50	100	45	15	45	60	35	20	20	45	35	-
AF	-	-	45	65	15	-	-	-	-	45	75	-	-	50	60	-	-	60	70
PF	-	-	5	30	-	-	-	-	-	10	10	-	5	15	20	-	-	5	30

Tab. 2: Optical evaluation of H.A.Z. phases amounts (in vol. %). P.F. : proeutectoïd ferrite

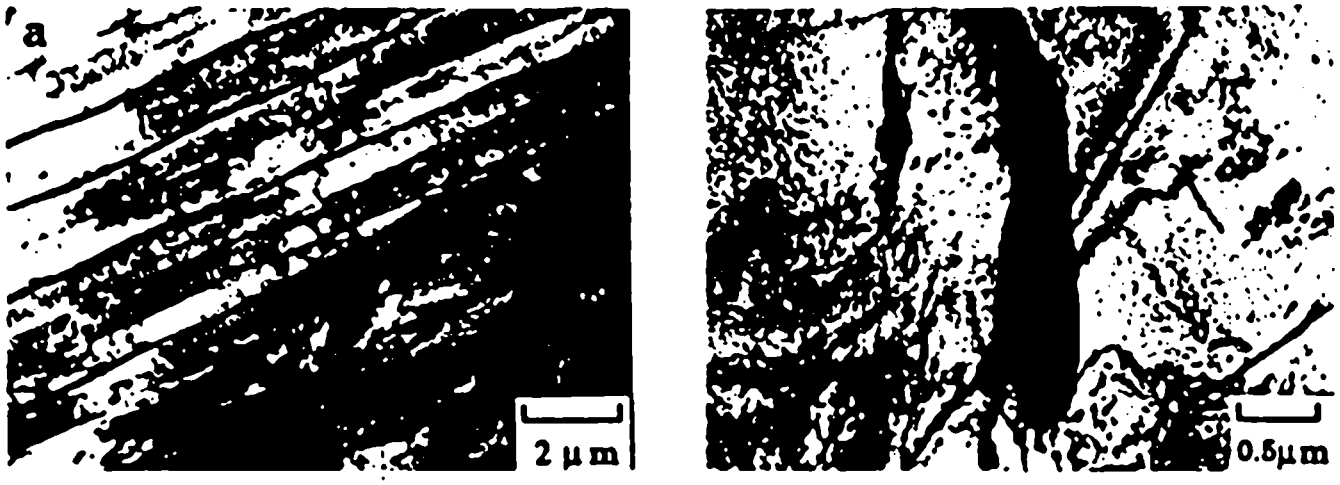

Fig. 2: M.A.C. aspect : a) interlath particles of retained austenite in steel I (Δt=10s); b) partial decomposition of austenite into pearlite in steel VI (Δt=300s).

As previously reported (1,3,4), the M.A.C. constituent is composed essentially of elongated interlath particles in lath upper bainite and of blocky pieces in acicular ferrite. It is noteworthy that this retained austenite (γ) is partially transformed into pearlite for the highest heat input (Fig. 2b), and into twinned martensite for the lowest welding energy. In accordance with these transformations, both X-ray diffractometry and Mössbauer spectrometry (Fig. 3) indicate that the austenite volume fraction evolves with Δt between 2 and 8.5 % (Fig. 4 and 5). The X-ray data arise from the ratio of the integrated

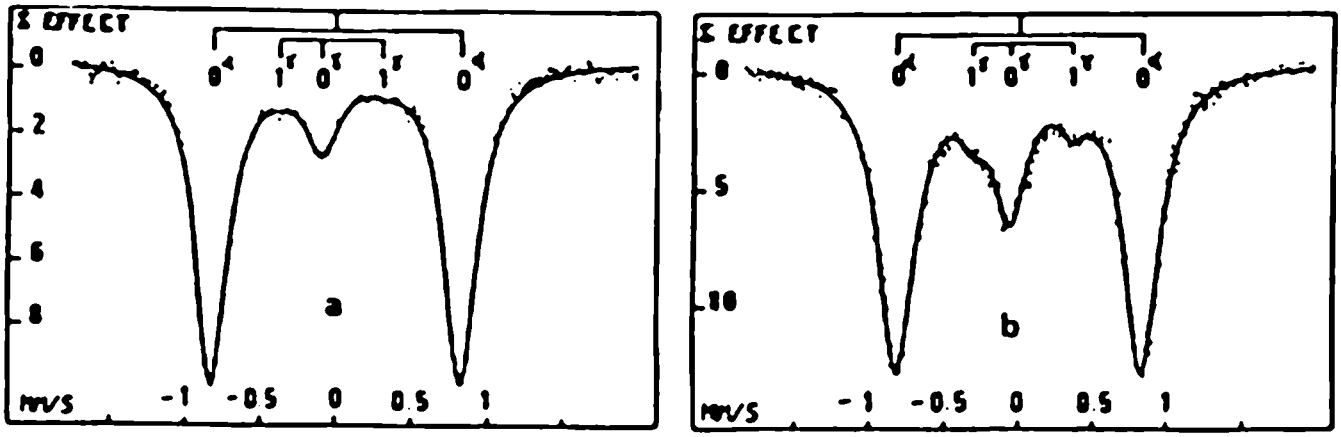

Fig. 3: Mössbauer spectra of alloy I cooled at a) Δt=10s; b) Δt=100s.

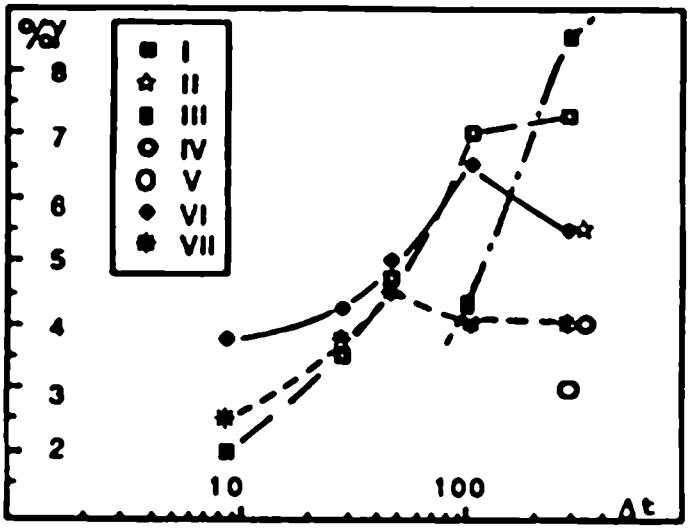

Fig. 4: X-ray estimate of the retained austenite content for the seven steels.

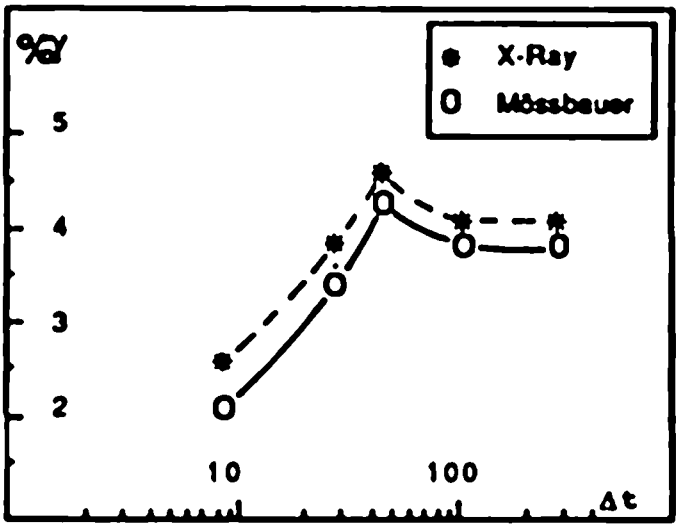

Fig. 5: Comparison of the X-ray and Mössbauer measurements of the retained austenite amount for steel VII

intensities of the $(200)_\alpha$ and $(111)_\gamma$ diffraction peaks (5). At the ± 2 mm.s^{-1} speed range, the Mössbauer spectra display the two middle peaks of ferrite and three peaks of austenite corresponding to the O^γ and I^γ iron atoms surroundings (Fig. 3). The O^γ and I^γ surroundings are defined respectively by the missing and by the presence of one atom in the sphere of the iron nearest interstitial neighbours. The details of the Mössbauer spectra treatment can be found in reference (6). The integration of the austenite and ferrite (α) peaks areas over both ± 9 mm.s^{-1} and ± 2 mm.s^{-1} speed ranges lead to the texture-free Mössbauer estimate of the γ volume fraction. Fig. 5 shows that these Mössbauer values are very close but lower than the X-ray results.

This small discrepancy may arise both from the neglect of the sample thickness effect and from the uncertainty in the Lorentzian peak deconvolution of the Mössbauer spectra. Moreover, it is worth emphasizing that, in comparison with X-ray diffractometry, Mössbauer spectrometry has the advantage of measuring the residual austenite carbon content $(\% C)_\gamma$. Fig. 6 indicates that $(\% C)_\gamma$ is included between 0.2 and 0.7 wt % and thus rather high according to the mean alloy composition. This carbon level depends both on the autenite stability and on the welding energy. The S.T.E.M. E.D.X. spectra show that, regarding their contents in substitutional atoms (Mn, Ti and Si), retained austenite and ferrite have the same composition.(1,4). The austenite stability is nevertheless achieved by the alloy chemistry that acts on its carbon enrichment. Using a Hultgren extrapolation of the equilibrium phase diagram, the carbon composition of the stable austenite will be the higher, the lower is the bainite transformation finishing temperature (3,4). Furthermore, and as illustrated by the alloy VII case, the residual austenite carbon content decreases during its pearlitic destabilization. Otherwise, as long as the austenite remains undecomposed in a steel, $(\% C)_\gamma$ increases with Δt, and then with the diffusion time. In summary, the evolutions shown in Fig. 4, of the volume fraction of austenite with Δt are explained by the competition between the austenite stabilization owing to its carbon enrichment, and its destabilization because of alloy composition.

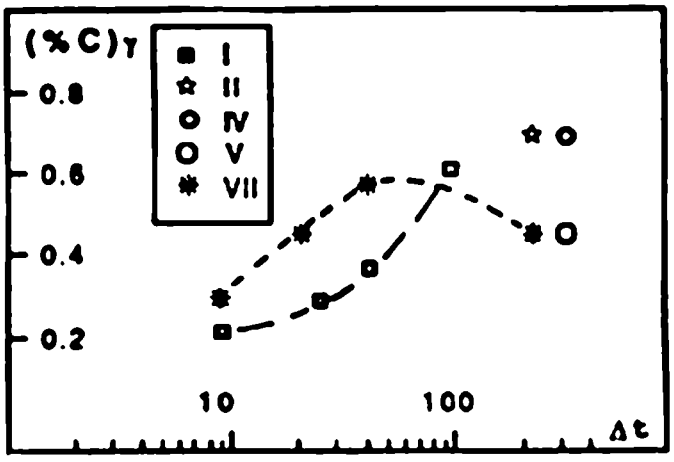

Fig. 6 : Evolution of $(\% C)_\gamma$ with Δt.

2. Effect of microstructure on H.A.Z. toughness

Among the numerous parameters a priori likely to operate on the toughness behaviour (N interstitial content, prior austenite grain size, precipitation, types of microstructural constituents...) the nature of the microstructure is the only one which exerts a significant influence in the present materials (3,4). Fig. 1b displays the relationship between T_K and the major microstructural constituents. The H.A.Z. toughness reduction with the welding energy has already been correlated with

its microstructure evolution from martensite to lower bainite and finally to lath upper bainite (7). It is noteworthy that the same feature is observed in the present work with alloys I and III at $\Delta t<50s$. In contrast, at higher Δt values the toughness-microstructure correlation is less known. However, according to Fig.1b, lath upper bainite structures exhibit the worst resilience, whereas the toughness seems improved by the amount of acicular ferrite. This feature can be explained by the effective grain size (De) concept of Naylor (8). For instance, the evaluation of De in lath upper bainite and in acicular ferrite leads to 7 µm and 3 µm in alloys II, IV and V. However, it should be noticed that the previous interpretation is insufficient in order to understand the T_K differences among the alloys at constant microstructure. The very harmful influence of residual austenite on toughness must be considered to overcome this difficulty. Fig. 7 shows that T_K increases by $14K/\gamma\%$ in a predominantly ferritic side plates structure (martensite and/or lath upper bainite) and only by $8K/\gamma\%$ in prevalence of acicular ferrite. It is worth noting that this detrimental influence is higher than the 8K/M.A.C. % reported by Kasamatsu (7) for lath upper bainitic structures. Moreover, Ikawa (9) has noticed that the detrimental effect of M.A.C. in alloyed steels is more efficient for high than for slow cooling rates. Furthermore, as illustrated by Fig. 8, retained austenite promotes both initiation and propagation of the fracture. These mechanical test data are checked by numerous observations of cavities at the M.A.C. interfaces (3) and by the crack route between the cavities. In the same way, Chen (10) has demonstrated the predominant effect of M.A.C. on crack initiation.

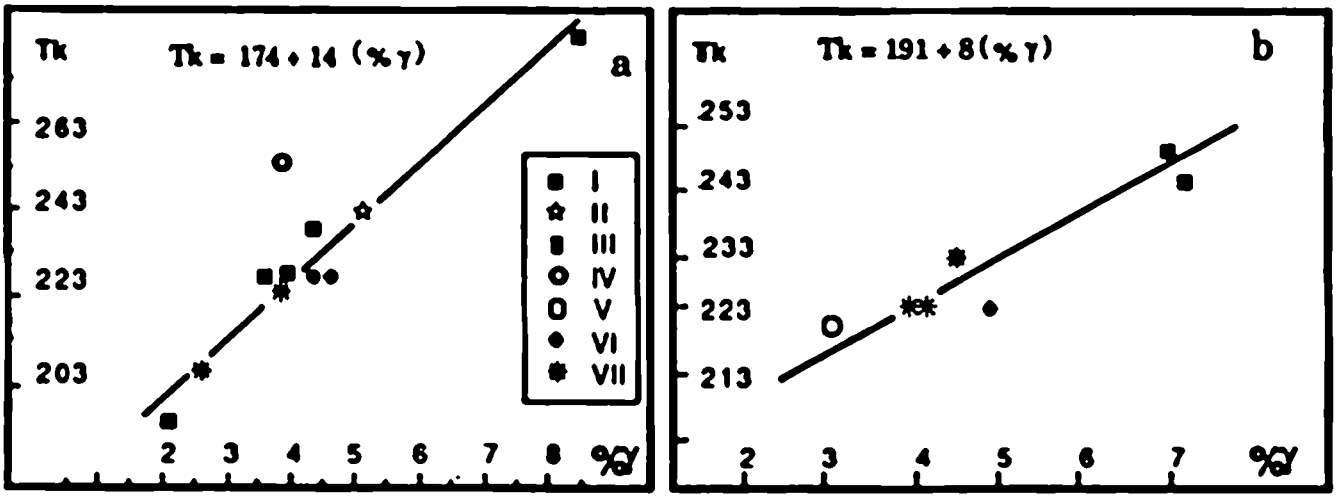

Fig. 7: Effect of retained austenite on T_K : a) lath microstructure, b) acicular microstructure.

Otherwise, according to Fig. 7a, the steel IV toughness is worse than it can be expected from its content in retained austenite. This discrepancy can only be explained by the existence of a significant volume fraction of proeutectoid ferrite (Tab. 2). The magnitude of the influence of a proeutectoid

ferrite net in bainite seems to arise from the plasticity variation between the softer allotriomorph net and the harder grain interior. So, it is worth noting that this harmful effect of proeutectoid ferrite is more marked in a ferrite side plates structure (steel IV) than in acicular ferrite (steel VII) because of their respective hardness.

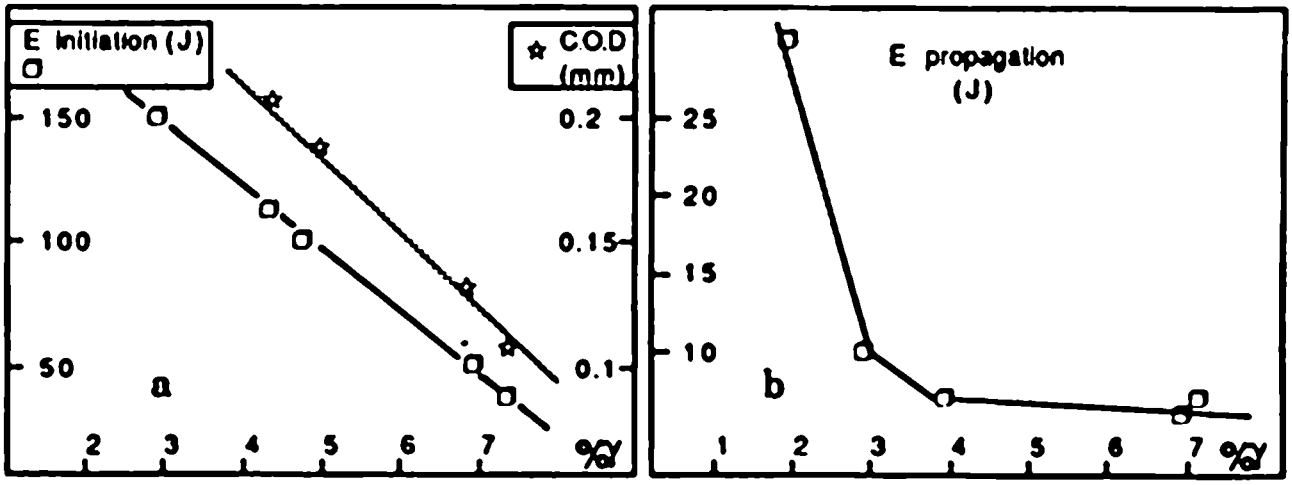

Fig. 8: Steel I tested at 243K. Unfavourable effect of γ on : a) the fracture initiation (C.O.D. + Charpy V); b) the fracture propagation (Charpy V data).

Conclusion

Mössbauer spectrometry and X-ray diffractometry show that the heat-affected zone of 0.1 wt % C microalloyed steels can contain up to 8.5 % in volume fraction of retained austenite. This austenite content depends both on the steels chemical composition and on the welding cooling time. The Mössbauer - estimated carbon level in austenite is monitored by the finishing bainite transformation temperature, the cooling time and the trend towards a pearlitic destabilization.

By comparison with the various parameters a priori likely to act on toughness properties, residual austenite exerts a significant and harmful effect. The Charpy V transition temperature increases by 14K/γ% and by 8K/γ% respectively in a ferritic side plates and in an acicular ferritic structure. The results of the mechanical tests and of the metallographic observations show that residual austenite promotes both the crack nucleation and propagation.

Otherwise, at high heat inputs, the best H.A.Z. toughness is achieved for an acicular ferritic structure. Moreover, a deleterious influence of proeutectoid ferrite is noted when associated with lath upper bainite.

References

(1) R. Taillard, T. Maurickx, J. Foct : "EMAG" 1985, Institute of Physics Conf. 78 (1985) 391.

(2) T. Maurickx, R. Taillard : "High Nitrogen Steels" 88, Institute of Metals, to be published.
(3) P. Verrier, T. Maurickx, R. Taillard, G. Garrigues : "Offshore Mechanics and Arctic Engineering" 1989, ASME, to be published.
(4) T. Maurickx, Doctoral Thesis, Université de Lille I, (1987) n°411.
(5) P. Guiraldenq, VIème Journée des Aciers Spéciaux, Société Française de Métallurgie 1967.
(6) T. Maurickx, R. Taillard, J. Foct : C.R. Acad. Sc. Paris. 303 Série II (1986) 41.
(7) Y. Kasamatsu, S. Takashima, T. Hosoya : J. Iron Steel Inst. Jap. 65 (1979) 92.
(8) J.P. Naylor, Doctoral Thesis, I.N.P. Lorraine, Nancy (1976) A.O. 12.278.
(9) H. Ikawa, H. Oshige, T. Tanoue : Trans. Jap. Weld. Soc. 11 (1980) 3.
(10) J.H. Chen, Y. Kikuta, T. Araki, M. Yoneda, Y. Matsuda : Act. Met. 32 (1984) 1779.